Chemistry & Biology
Article

Polyketide β-Branching in Bryostatin Biosynthesis: Identification of Surrogate Acetyl-ACP Donors for BryR, an HMG-ACP Synthase

Tonia J. Buchholz,[1] Christopher M. Rath,[1,2] Nicole B. Lopanik,[1,5] Noah P. Gardner,[1,2] Kristina Håkansson,[2] and David H. Sherman[1,2,3,4,*]
[1]Life Sciences Institute
[2]Department of Chemistry
[3]Department of Medicinal Chemistry
[4]Department of Microbiology and Immunology
University of Michigan, Ann Arbor, MI 48109, USA
[5]Present address: Department of Biology, Georgia State University, Atlanta, GA 30303, USA
*Correspondence: davidhs@umich.edu
DOI 10.1016/j.chembiol.2010.08.008

SUMMARY

In vitro analysis of natural product biosynthetic gene products isolated from unculturable symbiotic bacteria is necessary to probe the functionalities of these enzymes. Herein, we report the biochemical characterization of BryR, the 3-hydroxy-3-methylglutaryl (HMG)-CoA synthase (HMGS) homolog implicated in β-branching at C13 and C21 of the core ring system from the bryostatin metabolic pathway (Bry). We confirmed the activity of BryR using two complementary methods, radio-SDS PAGE, and Fourier transform ion cyclotron resonance-mass spectrometry (FTICR-MS). The activity of BryR depended on pairing of the native acetoacetyl-BryM3 acceptor acyl carrier protein (ACP) with an appropriate donor acetyl-ACP from a heterologous HMGS cassette. Additionally, the ability of BryR to discriminate between various ACPs was assessed using a surface plasmon resonance (SPR)-based protein-protein binding assay. Our data suggest that specificity for a protein-bound acyl group is a distinguishing feature between HMGS homologs found in PKS or PKS/NRPS biosynthetic pathways and those of primary metabolism. These findings reveal an important example of molecular recognition between protein components that are essential for biosynthetic fidelity in natural product assembly and modification.

INTRODUCTION

The bryostatins are antifeedant polyketide natural products produced by a bacterial symbiont of the marine bryozoan *Bugula neritina* (Sudek et al., 2007). They are highly potent protein kinase C (PKC) modulators (Nelson and Alkon, 2009), and, as such, bryostatin 1 (Figure 1) has been investigated in numerous clinical trials as a potential anticancer agent (Banarjee et al., 2008). Separately, the neuroprotective activity of PKC activators has recently been demonstrated in preclinical studies where bryostatin 1 was able to rescue memory loss after postischemic stroke (Sun et al., 2009). Additional studies suggest that bryostatin 1 (and a synthetic analog) may be able to reduce the levels of Aβ, a toxic peptide implicated in Alzheimer's disease (Khan et al., 2009; Nelson et al., 2009). However, like many marine-derived natural products, fulfilling the promise of these initial studies may be hindered by the low abundance of bryostatins available from either natural sources or chemical synthesis (Sudek et al., 2007; Singh et al., 2008). The intriguing biological activities and lingering supply questions motivate our continued study of the bryostatin biosynthetic pathway (Figure 1). Increasing our knowledge of the molecular mechanisms employed may help open the door to new methods of bryostatin production as well as the generation of related bryostatin analogs. Herein, we report the biochemical characterization of BryR, the 3-hydroxy-3-methylglutaryl (HMG)-CoA synthase (HMGS) homolog implicated in β-branching at C13 and C21 of the core bryostatin ring system (Figures 1 and 2).

Polyketide metabolites are produced by diverse bacterial taxa, including soil-dwelling bacteria, cyanobacteria, and bacterial symbionts living within insects or marine invertebrates, and are all generated by decarboxylative condensation reactions of simple coenzyme A (CoA) building blocks (Staunton and Weissman, 2001; Weissman, 2009; Hertweck, 2009). Polyketides with variable levels of reduction at the β-ketone position are built by type I polyketide synthases (PKSs). Type I PKSs are composed of a linear arrangement of covalently fused catalytic domains within large, multifunctional proteins. A unidirectional assembly line process is used to generate a linear intermediate that is often off-loaded as a cyclized lactone product. Sets of domains grouped together to accomplish a single round of extension are termed modules. The number, arrangement, and architecture of modules within type I systems serve as a blueprint to determine the core structure of the natural product (Weissman, 2009; Smith and Tsai, 2007; Fischbach and Walsh, 2006).

While methylation at the α position relative to the carbonyl group is well characterized (Staunton and Weissman, 2001; Smith and Tsai, 2007), alkylation at the β position (e.g., β-branching) is less commonly observed but can introduce further

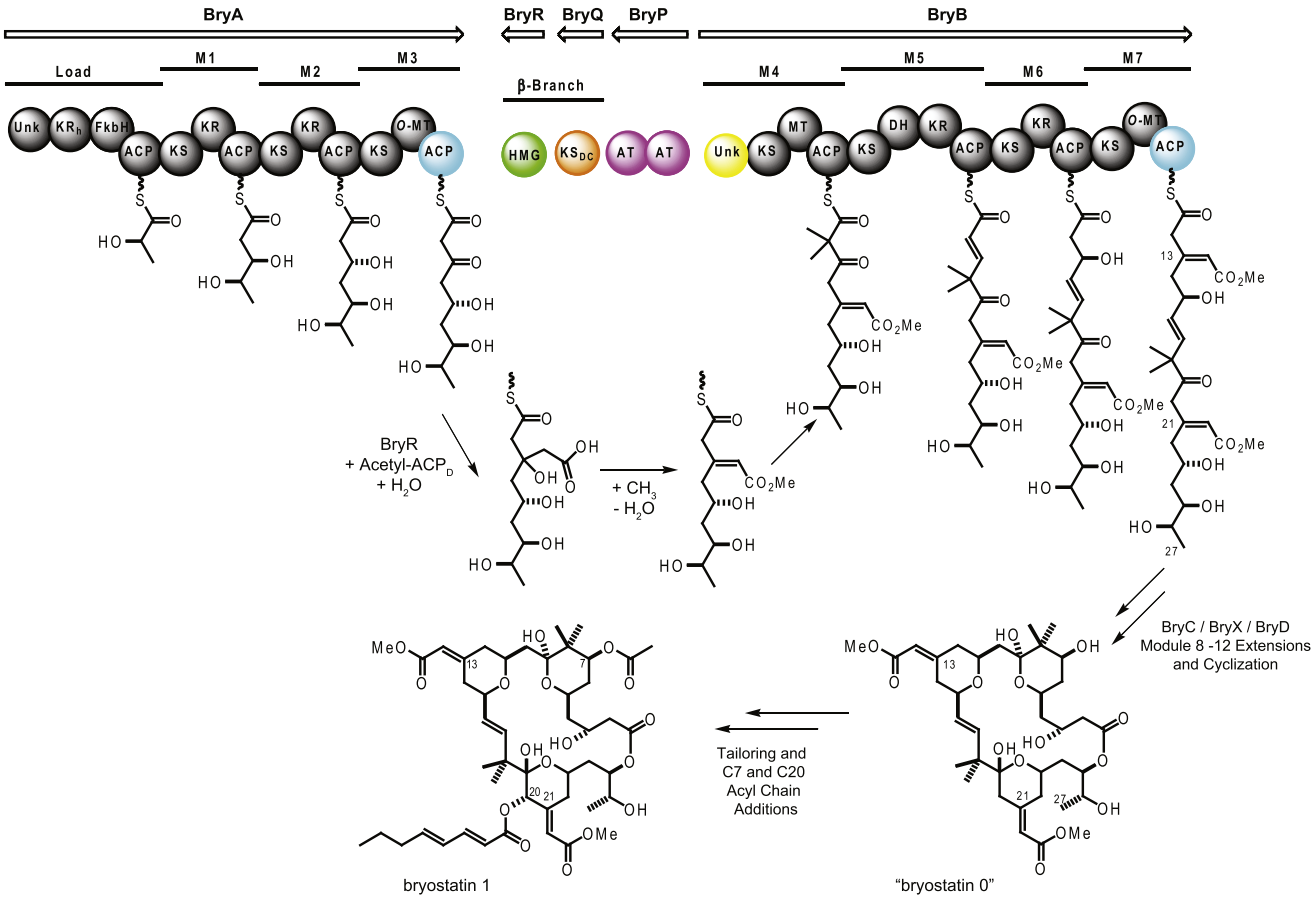

Figure 1. Portions of the Pathway Utilized in β-Branching Are Highlighted with Color in this Depiction of the Bryostatin Biosynthetic Pathway
BryC, BryX, and BryD are not shown (Sudek et al., 2007). Though the complete structure of the PKC modulator bryostatin 1 is shown here, the full suite of bryostatin molecules contains acyl chain variability at both C7 and C20. ACP, acyl carrier protein; AT, acyltransferase; DH, dehydratase; FkbH, homolog to FkbH (Wu et al., 2000); HMGS, HMG-CoA synthase homolog; KR, ketoreductase; KS, ketosynthase; KS_{DC}, decarboxylative ketosynthase; MT, methyltransferase; Unk, domain with unknown function. Refer to Figure S1 for more information.

functional group complexity into polyketides. Significant genetic and biochemical evidence has been obtained to demonstrate that β position alkyl side chains are typically introduced through an "HMGS cassette" of enzymes/domains performing reactions similar to those observed in mevalonate biosynthesis (Figures 2A and 2B) (Calderone et al., 2006, 2008; Geders et al., 2007; Gu et al., 2006; Simunovic and Müller, 2007a, 2007b). This set of enzymes typically contains three discrete proteins; the HMGS homolog, a decarboxylative ketosynthase (Cys to Ser active site variant, KS_{DC}), and a donor acyl carrier protein (ACP_D) upon which acetyl-ACP_D (Ac-ACP_D) is typically generated. Additionally, one or two enoyl-CoA hydratase (ECH) homologs responsible for dehydration and decarboxylation transformations (ECH_1 and ECH_2, respectively) may be present as discrete proteins or embedded domains in larger, multifunctional proteins (Figure 2B; see Figure S1 available online). Finally, many of the pathways contain tandem acceptor ACPs (ACP_A) at the site of modification. Full HMGS cassettes have been shown to install methyl branch points in bacillaene, curacin, jamaicamide, and mupirocin (Geders et al., 2007; Gu et al., 2006; Calderone et al., 2006; Wu et al., 2007), and hypothesized for methylation in pederin (Piel et al., 2004), and virginiamycin M (Pulsawat et al., 2007). Methoxymethyl and ethyl branches are added to the growing myxovirescin molecule in a similar fashion (Simunovic and Müller, 2007b; Calderone et al., 2007). However, the identity of the AT/KS pair responsible for generating the propionyl-ACP_D remains unconfirmed (Liu et al., 2009). In some cases, the methyl branch points are elaborated further by neighboring domains (the action of the nearby halogenase and enoyl reductase domains convert the β position in the mature curacin to a cyclopropyl ring while jamaicamide contains a vinyl chloride) (Gu et al., 2009; Figure S1). One notable exception to the HMGS-mediated chain-branching strategy was recently found in the rhizoxin biosynthetic pathway where a PKS-mediated Michael addition is employed in the generation of a δ-lactone (Kusebauch et al., 2009).

Partial HMGS cassettes have been identified in the onnamide, difficidin, psymberin, leinamycin (Piel et al., 2004; Liu et al., 2009; Chen et al., 2006; Fisch et al., 2009), and bryostatin (missing ACP_D, ECH_1 & ECH_2) (Sudek et al., 2007) biosynthetic pathways (Figure S1). Lack of complete gene cluster sequencing or annotation is one possible explanation for the presence of a partial

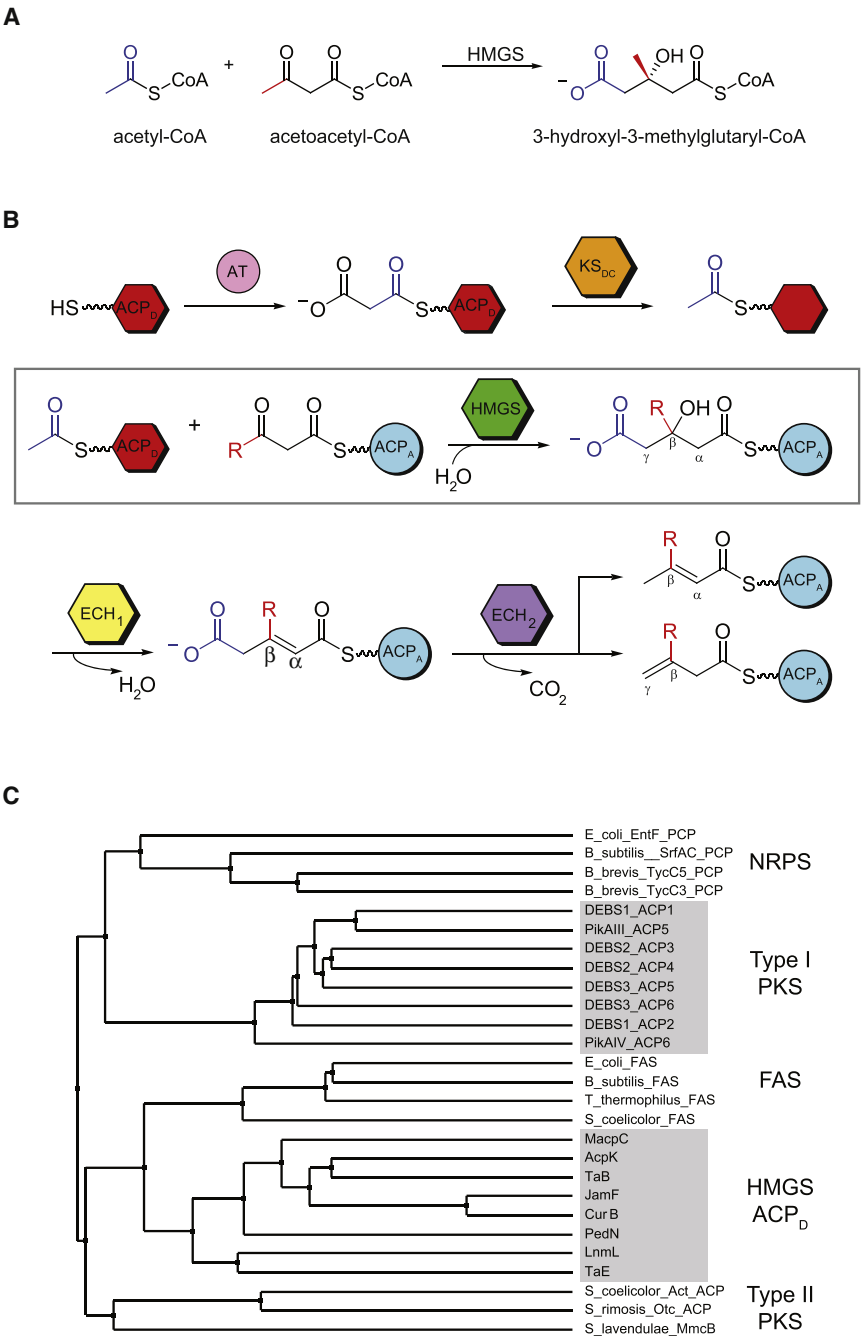

Figure 2. Proteins and/or Domains Involved in HMG Generation

(A and B) (A) HMG generation in the mevalonate pathway and (B) during polyketide β-branching in PKS and mixed biosynthetic pathways. The covalent, enzyme-bound intermediate from the reaction being analyzed in this paper is boxed.

(C) The HMGS cassette ACP_D subclass of acyl carrier proteins can be observed in the phylogenetic tree generated using Jalview software (average distance BIOSUM2) (Clamp et al., 2004). Refer to Figure S2 for more information.

HMGS cassette. This is likely the case for the onnamide, virginiamycin, difficidin, and bryostatin systems where boundaries have yet to be determined for contiguous pathways or the pathway is possibly dispersed across the genome. In other instances (leinamycin, bryostatin), product formation is unlikely to involve enzymatic transformations by the ECH homologs (dehydration and decarboxylation). Alternately, functions performed by the canonical set of HMGS cassette members might be catalyzed by alternative domains/enzymes within the pathway. For example, the leinamycin pathway does not include a KS_{DC}, as LnmK fulfills this role as an acyltransferase/decarboxylase to generate the acyl donor propionyl-LnmL (Liu et al., 2009). Similarly, the β-methoxylacylidene moieties found in the bryostatins are hypothesized to be the result of a β-γ dehydration (whereas the dehydration performed by ECH_1 enzymes typically occurs across the α-β positions) (Calderone, 2008). The N-terminal domains of unknown function found on BryB and BryC are candidates to catalyze these transformations, found immediately downstream of both HMGS modification sites in the bryostatin pathway (Sudek et al., 2007).

The type I PKS biosynthetic gene cluster (*bry*) presumed responsible for the synthesis of the bryostatins has been identified and sequenced from two sibling unculturable bacterial symbiont species of "*Ca.* Endobugula sertula/*B. neritina*" (Sudek et al., 2007). The shallow-water North Carolina (NC) sibling species appears to be located within a contiguous DNA fragment approximately 77 kb in length, whereas the deep-water California (CA) species is split between two or more locations on the chromosome. Apart from the transposition of the HMGS cassette and AT enzymes, the two sequences exhibit >99.5% identity at the DNA level. In the current study, we have focused on BryR from the NC species of "*Ca.* Endobugula sertula/*B. neritina*" to elucidate its role in the β-branching process (e.g., formation of HMG-ACP) during bryostatin assembly.

The canonical HMGS cassette activities have been elucidated through in vitro biochemistry or in vivo gene disruption studies in the bacillaene, curacin/jamaicamide, and myxovirescin pathways (Calderone, 2008). A key step for selectivity in the HMGS cassette appears to be the HMGS reaction itself (Calderone et al., 2006). Biochemical studies of PksG, the HMGS homolog of the bacillaene pathway, revealed that the enzyme only accepts the acetyl group when presented on AcpK, its cognate ACP_D (Calderone et al., 2006). In addition, gene deletion studies

of the myxovirescin HMGS cassette enzymes indicate that the two HMGS homologs present (TaC/TaF) utilize separate ACP_Ds (TaB/TaE) (Simunovic and Müller, 2007a). The ability of PksG to accept a model substrate, acetoacetyl (Acac)-ACP_A, is consistent with the importance of protein-protein interactions for HMGS-ACP_D specificity (Calderone et al., 2006). The role of protein-protein interactions in mediating biosynthetic processes for polyketide β-branching, and its role in chemical diversification motivated our current studies, described below.

RESULTS AND DISCUSSION

Based on the reported activities of the previously characterized secondary metabolite HMGS homologs PksG and TaC (Calderone et al., 2006, 2007), BryR is likely to be involved in the β-branching at C13 and C21 of the bryostatins (Figures 1 and 2). To date, no discrete ACP for the HMGS cassette of the bryostatin pathway has been located in either the NC or CA *bry* cluster sequences. The possibility exists that BryR, like its primary metabolism counterparts, may be able to use acetyl-CoA as the acyl donor in its reaction (Calderone, 2008). However, the presence of a KS-type (BryQ) decarboxylase, whose presumed role is to generate acetyl-ACP from malonyl-ACP, makes this an unlikely scenario. A discrete ACP upstream of the *bry* cluster was identified adjacent to genes that encode proteins likely involved in fatty acid biosynthesis (Bry FAS ACP). Though other fatty acid synthase (FAS) ACPs have not been reported as part of HMGS cassettes, no other endogenous ACP_D candidates were evident in or near the *bry* cluster. Therefore, in the absence of a Bry ACP_D, we sought to identify surrogate acetyl donors for substrate loading of BryR.

Several types of ACPs were surveyed (discrete ACP_Ds from HMGS-cassettes, type II PKSs and bacterial FASs, and excised ACPs from type I PKSs) in search of suitable ACP_D partners for BryR (Figure 2C). The unmodified (apo-) and phosphopantetheine (PPant)-containing (holo-) forms of the ACPs were overexpressed in *Escherichia coli* and purified. The Ac- or Acac-modified ACPs were generated by loading the apo-ACPs in vitro using Sfp or Svp (flexible phosphopantetheinyl transferases [PPTases], respectively) (Lambalot et al., 1996; Sanchez et al., 2001). Modified ACPs were separated from unreacted CoAs before testing (see Supplemental Information). To assess the ability of BryR to catalyze HMG formation using the surrogate acyl carriers (Ac-ACP_D + Acac-ACP_A → HMG-ACP_A), we monitored the enzymatic activity of BryR when paired with different Ac-ACP_D and Acac-ACP_A substrates.

In primary metabolism, HMG-CoA synthase (HMGS) catalyzes the condensation of C2 of acetyl-CoA onto the β-ketone of acetoacetyl-CoA to form 3-hydroxyl-3-methylglutaryl-CoA and free CoASH (Lange et al., 2000; Steussy et al., 2005, 2006). A number of secondary metabolite pathways have been identified over the past 5 years that perform a similar reaction, although they appear to use ACP-tethered acyl groups as opposed to acyl-CoA substrates. By analogy to primary metabolism HMGSs, the first step in the BryR mechanism should be acetylation of the active site cysteine in the enzyme (Theisen et al., 2004). Subsequently, the C2 of acetate reacts with the β-keto group of the Acac-ACP_A substrate to form HMG (or a related molecule during biosynthesis) (Figures 2A and 2B). These steps were assessed by both Fourier transform ion cyclotron resonance mass spectrometry (FTICR-MS) (Figure 3A) and radio-SDS PAGE (Figure 3B). Substrate transfer from Ac-ACP (FTICR-MS) or [1-^{14}C]-Ac-ACP (radio-SDS PAGE) to BryR was confirmed only when a member of the discrete HMGS-cassette ACP_D group (Figure 2C) was paired with BryR (Figure 3). By FTICR-MS, we were also able to observe loss of the Ac-ACP_D species and its conversion to holo-ACP_D in the presence of BryR (Figure 3A; Figures S4–S7).

Generation of the Ac-BryR intermediate during the first half of the reaction can be visualized in the phosphorimage only when [1-^{14}C]-Ac-CurB (HMGS-cassette ACP_D) donates the acetyl group (Figure 3B). To confirm that the BryR reaction proceeds through the same enzyme intermediate as those observed in primary metabolism, we confirmed that the acetylation occurs on Cys114. BryR (10 μM) was reacted with Ac-MacpC (50 μM) in the absence of an ACP_A. After the sample was proteolyzed with trypsin, peptides were separated by HPLC, and using LC-FTICR MS and ion trap LC-MS/MS the BryR active site peptide was identified and acetylation of Cys114 was confirmed (Table 1). Additionally, a mutant form of the protein at this location (C114A) was enzymatically inactive (data not shown). These data represent the first direct demonstration of the Ac-Cys species in an HMGS homolog in polyketide biosynthesis.

As evidence of the ability of BryR to catalyze the complete reaction (Ac-ACP_D + Acac-ACP_A → HMG-ACP_A), we observed a third radioactive band, consistent with modification of BryM3 ACP (a model acceptor substrate), an embedded ACP excised from the BryA tetramodule at one of the predicted HMGS modification sites (Figures 1 and 3B). To identify the chemical modification on BryM3 ACP, the reaction mixtures were monitored by top-down FTICR-MS. The mass shift of +60.0 Da on the intact BryM3 ACP between the +/− BryR samples is consistent with conversion of the Acac-BryM3 ACP_A substrate to HMG-BryM3 ACP_A (Figure 3A). MS/MS analysis was performed using the PPant ejection assay (Dorrestein et al., 2006a, 2006b), which confirmed that the mass shift between +/− BryR samples is due to modification of the PPant prosthetic group. No product formation was observed when Ac-Bry FAS ACP was incubated with BryR and Acac-BryM3 ACP (data not shown). Other reactions without detectable product formation included an Ac-FAS ACP donor from *Streptomyces coelicolor* (SCO2389, *Sc* FAS ACP) (Arthur et al., 2009), an Ac-CoA donor, using BryM3 ACP as both donor and acceptor, or Acac-FAS ACPs or Acac-MacpC as acceptors (data not shown).

Since the HMGS homologs found in secondary metabolism do exhibit a preference for acyl-ACPs, we sought to measure the affinity of BryR for these ACPs. The direct binding of BryR to a variety of potential Ac-ACP_Ds as well as the model acetoacetyl acceptor substrate, Acac-BryM3 ACP was assessed (Figure 4). After BryR immobilization to a BIAcore CM5 SPR chip (Figure S10), equilibrium binding analysis was performed using sequential injections of apo-, holo-, Ac-, or Acac-ACPs at varying concentrations (Figure 4; Figure S11). Active BryR (WT) and an enzymatically inactive (C114A) BryR mutant behaved similarly in our binding studies. BryR was able to bind to ACP_Ds from the curacin (CurB), jamaicamide (JamF), and mupirocin (MacpC) HMGS cassettes as well as to the excised native acceptor (BryM3 ACP) (Figure S1). Affinities (K_Ds) were in the

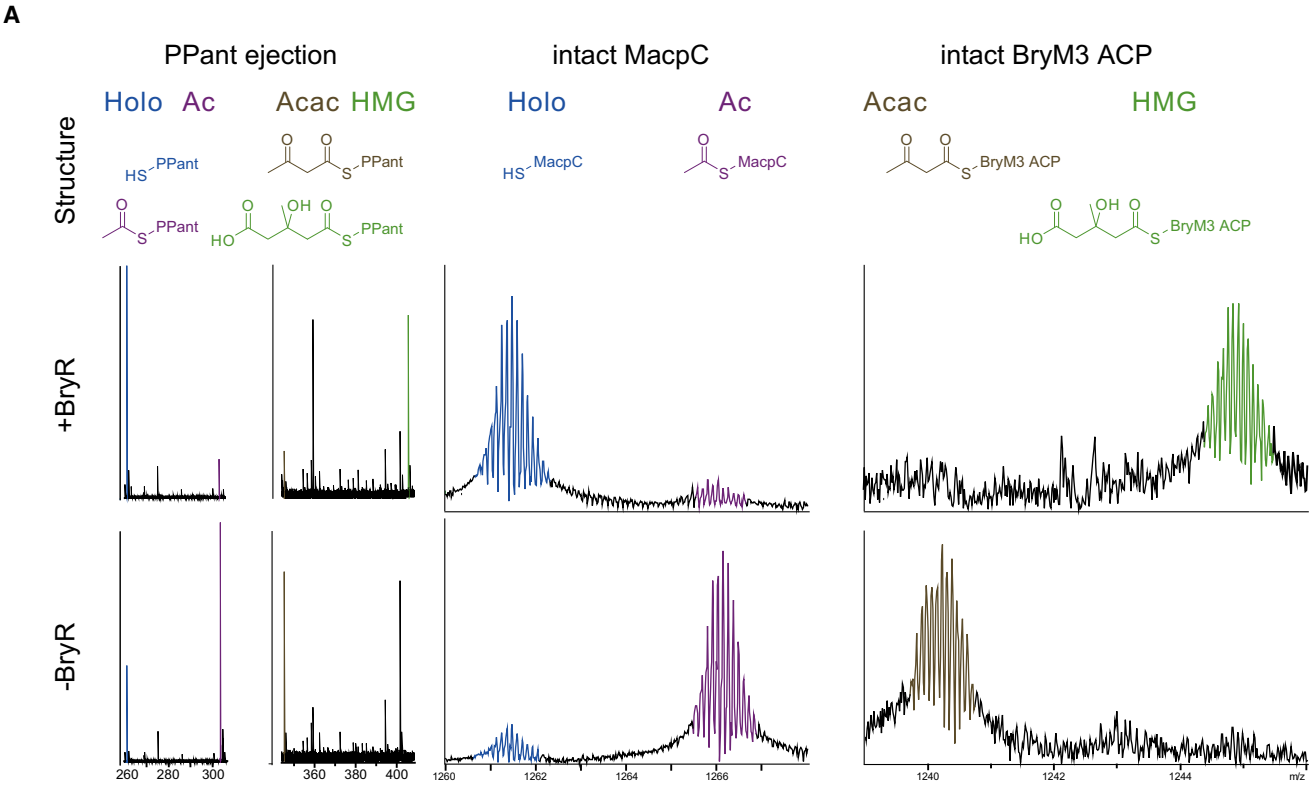

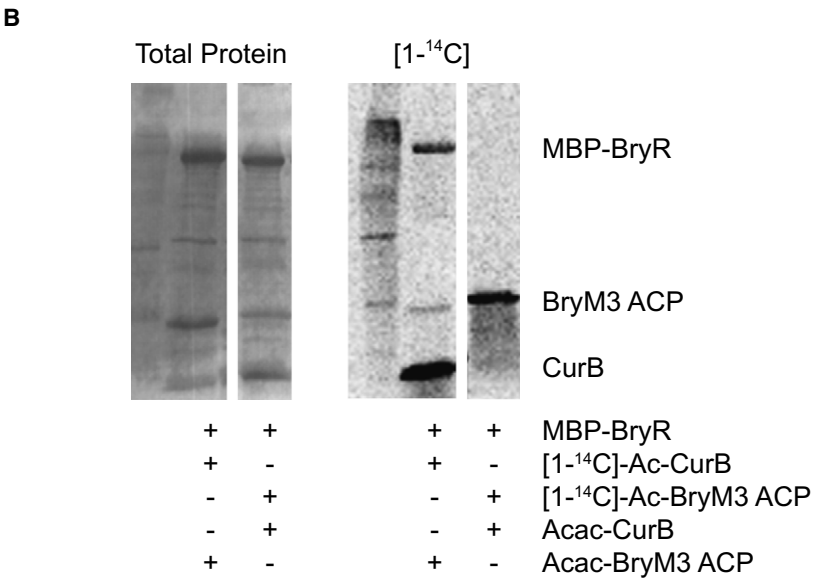

Figure 3. BryR Catalyzed Generation of HMG-BryM3 ACP from Ac-MacpC

(A) As monitored by FTICR-MS, data are presented as m/z (x-axis) versus abundance (y-axis). PPant ejection assay data from the entire charge state distribution are presented. PPant ejection peaks are in the +1 charge state. Intact donor and acceptor ACP data are also illustrated. Holo- and Ac-MacpC peaks are shown in the +13 charge state. Acac- and HMG-BryM3 are shown in the +14 charge state. Particular charge states illustrated are representative of the entire charge state envelope.

(B) Rado-TLC monitored acetyl transfer from [1-^{14}C]-Ac-CurB to Acac-BryM3 ACP to form HMG-BryM3 ACP monitored by radio-SDS PAGE.

Refer to Figures S4–S9 for more information.

Table 1. Ac-BryR Active Site Peptide Fragment Ions Observed in Ion Trap LC/MS/MS

Mass	Intensity	ID[a]	Δppm
480.18	62	a_4	−28
463.13	30	a_4 - NH_3	−65
567.19	18	a_5	−67
550.24	28	a_5 - NH_3	79
708.28	76	a_7 - NH_3	19
753.19	51	b_7	−132
735.22	451	b_7 - H_2O	−76
736.23	145	b_7 - NH_3	−37
824.28	22	b_8	−53
806.54	16	b_8 - H_2O	276
807.32	91	b_8 - NH_3	28
732.35	17	y_6 - NH_3	−70
749.30	21	y_6 - NH_3	−171
845.34	20	y_7 - NH_3	−172
1,064.52	18	y_9	−63
1,047.46	35	y_9 - NH_3	−104

[a] *b*- and *y*-type fragment ions originate from peptide backbone bond cleavage where *b* ions contain the peptide N terminus and *y* ions contain the peptide C terminus. The subscripted number indicates the number of amino acid residues in a particular fragment. *a*-type ions result from secondary fragmentation of *b* ions via CO loss.

middle to high micromolar range for ACP_Ds (40–110 μM) and the ACP_A (180 μM). The pattern of BryR binding affinities correlated well with that observed in our enzymatic activity assays. No significant binding was observed between Bry FAS ACP (up to 500 μM) or *Sc* FAS ACP (up to 650 μM) and BryR (Figure 4B). No enhancement of affinity was observed between apo- and Ac-ACP_D or between apo-, holo-, Ac-, AcAc-, or HMG-ACP_A (Figure 4B). Thus, the affinity of BryR for the ACPs seems to be mediated mainly by protein-protein contacts (as opposed to protein-acyl chain or protein-PPant contacts). These data suggest that specificity for a protein-bound acyl group is a distinguishing feature between HMGS homologs found in PKS or mixed PKS/nonribosomal peptide synthase (NRPS) biosynthetic pathways and those of primary metabolism.

SIGNIFICANCE

We have investigated the enzymatic function of BryR (condensation of acetyl-ACP_D with acetoacetyl-ACP_A to form HMG-ACP_A) using two complementary methods, radio-SDS PAGE and FTICR-MS. The activity of BryR was dependent on pairing of the native Acac-BryM3 acceptor ACP with an appropriate surrogate Ac-ACP_D from a related HMGS cassette (CurB, JamF, or MacpC). In addition, the ability of BryR to discriminate between various ACPs was assessed using an SPR-based protein-protein binding assay. BryR bound selectively to ACPs obtained from a series of HMGS cassettes (MacpC, CurB, JamF, and BryM3 ACP). To date, no structural insights have been reported for the interaction of HMGS cassette enzymes with partner ACP_Ds. These future studies will be essential to determine the nature of BryR's ACP binding selectivity. Finally, this work, as well as other recent studies (Fisch et al., 2009; Lopanik et al., 2008) demonstrates further that natural product biosynthetic genes isolated from unculturable marine symbiotic bacteria can be manipulated in vitro in order to probe the functionalities of these enzymes from previously inaccessible sources.

EXPERIMENTAL PROCEDURES

Expression and Purification of Proteins

Plasmids encoding N-terminal His_6- or His_6/MBP- fusion protein tags were transformed into *E. coli* BL21(DE3) and grown at 37°C in TB medium to an OD_{600} of ~1.0 in 2 liter flasks. The cultures were cooled to 18°C, and isopropyl β-D-thiogalactopyranoside was added to a final concentration of 0.2 mM and grown 12–16 hr with shaking. The cells were harvested by centrifugation and frozen at −20°C. Cell pellets were thawed to 4°C and resuspended in 5X volume of lysis buffer (20 mM HEPES [pH 7.8], 300 mM NaCl, 20 mM imidazole, 1 mM $MgCl_2$, 0.7 mM Tris [2-carboxyethyl] phosphine [TCEP], ~100 mg CelLytic Express [Sigma-Aldrich]) before lysis via sonication. Centrifugation at 25,000 × g for 30 min provided clarified lysates. Proteins were purified using Ni-Sepharose affinity chromatography on an Akta FPLC. In brief, after filtration of the supernatant through 0.45 μm membrane, the solution was loaded onto a 5 ml HisTrap nickel-nitrilotriacetic acid column. The column was washed with ten column volumes of buffer A (20 mM HEPES [pH 7.8], 300 mM NaCl, 20 mM imidazole, 0.7 mM TCEP) and eluted with a linear gradient of buffer B (20 mM HEPES [pH 7.8], 300 mM NaCl, 400 mM imidazole, 0.7 mM TCEP). For ACP purifications, fractions were pooled, concentrated, and loaded onto a HiLoad 16/60 Superdex 75 (GE Healthcare Life Sciences) column equilibrated with storage buffer (20 mM HEPES [pH 7.4], 150 mM NaCl, 0.7 mM TCEP). Fractions were combined, concentrated, frozen, and stored at −80°C. Because some of the acyl carrier proteins lack amino acids with appreciable absorbance at 280 nm, protein concentrations were determined via the bicinchoninic acid (BCA) method using BSA as a standard. BryR purifications differed from ACP purifications in that all buffers contained 10% glycerol in addition to the components listed above. In addition, for SPR and FTICR-MS assays, His-MBP-tag removal was achieved by TEV protease incubation overnight at 4°C in buffer A. TEV protease and the N-terminal His-MBP tag were removed by repassaging the solution over the HisTrap column. Flow-through fractions were pooled, concentrated, and loaded onto a HiLoad 16/60 Superdex 200 column equilibrated with BryR storage buffer (10% glycerol, 20 mM HEPES [pH 7.4], 150 mM NaCl, 0.7 mM TCEP). Fractions were combined, concentrated, frozen, and stored at −80°C. Protein concentrations were determined using absorbance at 280 nm and calculated extinction coefficients (1 A_{280} = 1.2 mg/ml). ACPs were greater than 95% pure following the above purification. Typical yields for BryR batches were ~3 mg/liter of cell culture. TEV-cleaved BryR was approximately 85%–90% pure. Purity estimates are based on SDS-PAGE (Figure S3).

Enzymatic Analysis of BryR via Radio-TLC

Radiolabeled and unlabeled acyl-CoA substrates were transferred onto the various ACPs using Svp, a phosphopantheine transferase (PPTase) from *Streptomyces verticillus* (Sanchez et al., 2001). Acyl-CoAs (500 μM) were combined with 75 μM ACPs (CurB, BryM3 ACP) and 5 μM Svp in a Tris buffer (pH 7.4) containing $MgCl_2$ (10 mM) and DTE (1 mM), and the reaction proceeded for 1 hr at room temperature. The substrate-bound ACPs were desalted and utilized for experiments with BryR. The purified acylated donor (15 μM) and acceptor ACPs (30 μM) were incubated with BryR (10 μM) in 25 mM Tris buffer (pH 7.4) with DTE (1 mM) at room temperature for 5 min. Reactions were quenched by the addition of SDS-PAGE gel loading buffer. Samples were separated on polyacrylamide gels by SDS-PAGE. The gels

A

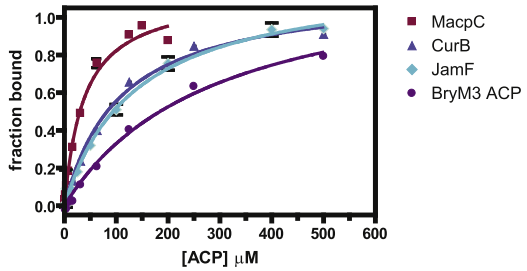

B

		apo-	*holo*-	Ac-	Acac-	HMG-
ACP_D	MacpC	40 ± 5 μM		32 ± 9 μM		
	CurB	108 ± 7 μM		90 ± 8 μM		
	JamF	100 ± 20 μM		107 ± 7 μM		
ACP_A	BryM3 ACP	177 ± 7 μM	180 ± 24 μM	200 ± 12 μM	150 ± 51 μM	170 ± 13 μM
	Bry FAS ACP	> 500 μM				
	Sc FAS ACP	> 650 μM				

Figure 4. Binding of apo-ACPs to Immobilized BryR, Monitored by SPR

(A) Each data point is the average of triplicate measurements; error bars are standard deviation. The data were fit to a one-site binding model ($Y = B_{max}*X/(K_D + X)$). Y = fraction bound, B_{max} = maximal response, X = ACP concentration. Dissociation constants (K_Ds) are reported in (B). Forms of ACPs shaded gray in the table were not tested. Refer to Figures S10 and S11 for more information.

were first stained using SimplyBlue (Invitrogen) and were then exposed to Phosphoimager screens. The screens were scanned using a Typhoon Scanner (GE Healthcare) and analyzed using ImageQuant.

Enzymatic Analysis of BryR via FTICR-MS

The preparation of acetyl-donor and acetoacetyl-acceptor ACPs was performed as above using Svp or Sfp PPTases(Lambalot et al., 1996). Acylated-ACPs were separated from CoA substrates via Zeba desalting columns (Pierce) or overnight dialysis in 3.5 kDa Slide-a-lyzer MINI dialysis units (Pierce) into 20 mM HEPES (pH 7), 150 mM NaCl. BryR (10 μM) was reacted with acetyl-donor ACP (50 μM) and acetoacetyl-acceptor ACP (80 μM) 75 mM HEPES (pH 7.5) buffer and 1 mM TCEP. After incubation for 60 min at room temperature, samples were acidified with 1% formic acid. Intact protein samples were desalted with Handee Microspin columns (Pierce) packed with 20 μl of 300 Å polymeric C4 resin (Vydac). Samples were loaded onto the columns and washed with 30 column volumes of 0.1% formic acid prior to elution with 10 column volumes of 50% acetonitrile plus 0.1% formic acid. Intact protein samples were analyzed by an FTICR MS (APEX-Q with Apollo II ion source and actively shielded 7T magnet; Bruker Daltonics). Data were gathered from m/z 200–2000 utilizing direct infusion electrospray ionization in positive ion mode. Electrospray was conducted at 3600 V with 24–60 scans per spectrum utilizing 0.5 s external ion accumulation in a hexapole and 15 ICR cell fills prior to excitation and detection. Collision cell pressure was reduced to 2.5e-6 Torr for improved transmission of protein ions. Infrared multiphoton dissociation (IRMPD) MS/MS was performed in the FTICR cell. This approach is preferred over external collision induced dissociation, because time-of-flight effects during ion transport into the FTICR cell are avoided. The laser power was 10 W with an irradiation time of 0.05–0.25 s. The entire mass range was fragmented, without any prior mass selection. Data were processed in Data Analysis (Bruker Daltonics) and Midas (NHMFL). All mass shifts shown were confirmed across all charge states for each ACP present. An abundant charge state is used for Figure 3 and Figures S4–S9 illustrate all charge states for the intact ions. All identified species were accurate to 20 ppm with external calibration. All experiments were performed at least twice to verify the findings.

Identification of BryR Active Site Acetylation by LC FTICR-MS and LC ion Trap-MS

BryR (10 μM) was reacted with acetyl-donor ACP (50 μM) and no acceptor ACP in 75 mM HEPES (pH 7.5) buffer, 1 mM TCEP. TPCK trypsin (1 mg/ml; Pierce) was added to a final 1:100 ratio. Samples were incubated at 37°C overnight. Twenty microliters of samples was injected onto a Jupiter C18 1 × 150 mm 300 μm column (Phenomenex) using an Agilent 1100 LC system with a flow rate of 75 μl/min and a gradient of 2%–98% acetonitrile over 85 min. Formic acid (0.1%) was added to the water and acetonitrile solvents. A divert valve was utilized for online desalting. The LC was coupled to an FTICR MS (APEX-Q with Apollo II ion source and actively shielded 7T magnet; Bruker Daltonics). Data were gathered from m/z 200–2000 in positive ion mode. Electrospray was conducted at 2600 V with four scans per spectrum utilizing 0.33 s external ion accumulation in a hexapole and 4 ICR cell fills prior to excitation and detection. Data were analyzed using DECON2LC and VIPER (Pacific Northwest National Labs). The acetylated active site peptide QA**C**YSGTAGFQMAINFILSR (2219.050 Da expected) was observed at 2219.045 Da representing a mass error of −2 ppm with external calibration. The same LC conditions were coupled to an LTQ Deca XP iontrap MS (Thermo). Online MS identified the same modified peptide, and online MS^2 allowed for confirmation that the modification occurred on the active site cysteine (Cys114) with the following fragment ions identified (Table 1). Data were processed in Excaliber version 3.0 (Thermo).

Surface Plasmon Resonance Assays of BryR, ACP_D, and ACP_A

Sensor chips (CM-5) and HBS-P buffer were purchased from GE Healthcare Life Sciences. SPR experiments were performed on a BIAcore 3000 instrument. Running buffer for SPR was HBS-P+T (10 mM HEPES [pH 7.4], 0.15 M NaCl, 0.005% surfactant P20, 50 μM TCEP). The surface was prepared for immobilization of BryR by activating with 70 μl of a fresh mixture of 0.2 M 1-ethyl-3-(3-dimethylaminopropyl)carbodiimide (EDC) plus 0.05 M *N*-hydroxysuccinimide at 10 μl/min. BryR diluted to 20 μM in 10 mM phosphate/citrate buffer (pH 5.5) and loaded at 5 μl/min (Figure S10). Typically, 1000–8000 RU of BryR was immobilized. Activated carboxy groups were blocked with 1 M ethanolamine/HCl (70 μl at 10 μl/min). The surface was regenerated with 10 μl of 50 mM NaOH, 1 M NaCl after immobilization and between ACP binding cycles. To measure binding to BryR by SPR, solutions of ACPs in HBS-P+T were injected over the prepared surface as well as an ethanolamine treated control flow cell at a flow rate of 10 μl/min. Baseline subtraction was performed using a mock-treated lane (activated with EDC/NHS and blocked with ethanolamine). Multiple injections (eight to ten concentrations) were tested in duplicate or triplicate. Maximum testable concentrations for the ACPs were limited by their solubility. Data analysis was carried out using BIAevaluation software (GE Healthcare Life Sciences). Representative sensorgrams for four concentrations of apo-JamF binding to BryR are shown in Figure S11. Nonlinear curve fitting of the equilibrium binding response was carried out using GraphPad Prism software.

SUPPLEMENTAL INFORMATION

Supplemental Information includes eleven figures and one table and can be found with this article online at doi:10.1016/j.chembiol.2010.08.008.

ACKNOWLEDGMENTS

We thank Christopher M. Thomas for the MacpC expression construct (pGTB340). C.M.R. received funding from the CBI training program (T32

GM008597) at the University of Michigan. This work was supported by NIH grant GM076477 and the Hans W. Vahlteich Professorship (to D.H.S.). N.B.L was supported by a National Institutes of Health NRSA fellowship (5F32CA110636). Work in K.H.'s laboratory is supported by an NSF Career Award (CHE-05-47699).

Received: June 10, 2010
Revised: August 10, 2010
Accepted: August 17, 2010
Published: October 28, 2010

REFERENCES

Arthur, C.J., Williams, C., Pottage, K., Płoskoń, E., Findlow, S.C., Burston, S.G., Simpson, T.J., Crump, M.P., and Crosby, J. (2009). Structure and malonyl CoA-ACP transacylase binding of *Streptomyces coelicolor* fatty acid synthase acyl carrier protein. ACS Chem. Biol. *4*, 625–636.

Banerjee, S., Wang, Z., Mohammad, M., Sarkar, F.H., and Mohammad, R.M. (2008). Efficacy of selected natural products as therapeutic agents against cancer. J. Nat. Prod. *71*, 492–496.

Calderone, C.T. (2008). Isoprenoid-like alkylations in polyketide biosynthesis. Nat. Prod. Rep. *25*, 845–853.

Calderone, C.T., Kowtoniuk, W.E., Kelleher, N.L., Walsh, C.T., and Dorrestein, P.C. (2006). Convergence of isoprene and polyketide biosynthetic machinery: isoprenyl-S-carrier proteins in the *pksX* pathway of *Bacillus subtilis*. Proc. Natl. Acad. Sci. USA *103*, 8977–8982.

Calderone, C.T., Iwig, D.F., Dorrestein, P.C., Kelleher, N.L., and Walsh, C.T. (2007). Incorporation of nonmethyl branches by isoprenoid-like logic: multiple β-alkylation events in the biosynthesis of myxovirescin A1. Chem. Biol. *14*, 835–846.

Chen, X.H., Vater, J., Piel, J., Franke, P., Scholz, R., Schneider, K., Koumoutsi, A., Hitzeroth, G., Grammel, N., Strittmatter, A.W., et al. (2006). Structural and functional characterization of three polyketide synthase gene clusters in *Bacillus amyloliquefaciens* FZB 42. J. Bacteriol. *188*, 4024–4036.

Clamp, M., Cuff, J., Searle, S.M., and Barton, G.J. (2004). The Jalview Java alignment editor. Bioinformatics *20*, 426–427.

Dorrestein, P.C., Blackhall, J., Straight, P.D., Fischbach, M.A., Garneau-Tsodikova, S., Edwards, D.J., McLaughlin, S., Lin, M., Gerwick, W.H., Kolter, R., et al. (2006a). Activity screening of carrier domains within nonribosomal peptide synthetases using complex substrate mixtures and large molecule mass spectrometry. Biochemistry *45*, 1537–1546.

Dorrestein, P.C., Bumpus, S.B., Calderone, C.T., Garneau-Tsodikova, S., Aron, Z.D., Straight, P.D., Kolter, R., Walsh, C.T., and Kelleher, N.L. (2006b). Facile detection of acyl and peptidyl intermediates on thiotemplate carrier domains via phosphopantetheinyl elimination reactions during tandem mass spectrometry. Biochemistry *45*, 12756–12766.

Fisch, K.M., Blackhall, J., Straight, P.D., Fischbach, M.A., Garneau-Tsodikova, S., Edwards, D.J., McLaughlin, S., Lin, M., Gerwick, W.H., Kolter, R., et al. (2009). Polyketide assembly lines of uncultivated sponge symbionts from structure-based gene targeting. Nat. Chem. Biol. *5*, 450–452.

Fischbach, M.A., and Walsh, C.T. (2006). Assembly-line enzymology for polyketide and nonribosomal peptide antibiotics: logic, machinery, and mechanisms. Chem. Rev. *106*, 3468–3496.

Geders, T.W., Gu, L., Mowers, J.C., Liu, H., Gerwick, W.H., Håkansson, K., Sherman, D.H., and Smith, J.L. (2007). Crystal structure of the ECH_2 catalytic domain of CurF from *Lyngbya majuscula*: insights into a decarboxylase involved in polyketide chain β-branching. J. Biol. Chem. *282*, 35954–35963.

Gu, L., Jia, J., Liu, H., Håkansson, K., Gerwick, W.H., and Sherman, D.H. (2006). Metabolic coupling of dehydration and decarboxylation in the curacin A pathway: functional identification of a mechanistically diverse enzyme pair. J. Am. Chem. Soc. *128*, 9014–9015.

Gu, L., Wang, B., Kulkarni, A., Geders, T.W., Grindberg, R.V., Gerwick, L., Håkansson, K., Wipf, P., Smith, J.L., Gerwick, W.H., et al. (2009). Metamorphic enzyme assembly in polyketide diversification. Nature *459*, 731–735.

Hertweck, C. (2009). The biosynthetic logic of polyketide diversity. Angew. Chem. Int. Ed. Engl. *48*, 4688–4716.

Khan, T.K., Nelson, T.J., Verman, V.A., Wender, P.A., and Alkon, D.L. (2009). A cellular model of Alzheimer's disease therapeutic efficacy: PKC activation reverses Abeta-induced biomarker abnormality on cultured fibroblasts. Neurobiol. Dis. *34*, 332–339.

Kusebauch, B., Busch, B., Scherlach, K., Roth, M., and Hertweck, C. (2009). Polyketide-chain branching by an enzymatic Michael addition. Angew. Chem. Int. Ed. Engl. *48*, 5001–5004.

Lambalot, R.H., Gehring, A.M., Flugel, R.S., Zuber, P., LaCelle, M., Marahiel, M.A., Reid, R., Khosla, C., and Walsh, C.T. (1996). A new enzyme superfamily—the phosphopantetheinyl transferases. Chem. Biol. *3*, 923–936.

Lange, B.M., Rugan, T., Martin, W., and Croteau, R. (2000). Isoprenoid biosynthesis: the evolution of two ancient and distinct pathways across genomes. Proc. Natl. Acad. Sci. USA *97*, 13172–13177.

Liu, T., Huang, Y., and Shen, B. (2009). Bifunctional acyltransferase/decarboxylase LnmK as the missing link for beta-alkylation in polyketide biosynthesis. J. Am. Chem. Soc. *131*, 6900–6901.

Lopanik, N.B., Shields, J.A., Buchholz, T.J., Rath, C.M., Hothersall, J., Haygood, M.G., Håkansson, K., Thomas, C.M., and Sherman, D.H. (2008). In vivo and in vitro trans-acylation by BryP, the putative bryostatin pathway acyltransferase derived from an uncultured marine symbiont. Chem. Biol. *15*, 1175–1186.

Nelson, T.J., and Alkon, D.L. (2009). Neuroprotective versus tumorigenic protein kinase C activators. Trends Biochem. Sci. *34*, 136–145.

Nelson, T.J., Cui, C., Luo, Y., and Alkon, D.L. (2009). Reduction of beta-amyloid levels by novel PKCε activators. J. Biol. Chem. *284*, 34514–34521.

Piel, J., Hui, D., Wen, G., Butzke, D., Platzer, M., Fusetani, N., and Matsunaga, S. (2004). Antitumor polyketide biosynthesis by an uncultivated bacterial symbiont of the marine sponge *Theonella swinhoei*. Proc. Natl. Acad. Sci. USA *101*, 16222–16227.

Pulsawat, N., Kitani, S., and Nihira, T. (2007). Characterization of biosynthetic gene cluster for the production of virginiamycin M, a streptogramin type A antibiotic, in *Streptomyces virginiae*. Gene *393*, 31–42.

Sanchez, C., Du, L., Edwards, D.J., Toney, M.D., and Shen, B. (2001). Cloning and characterization of a phosphopantetheinyl transferase from *Streptomyces verticillus* ATCC15003, the producer of the hybrid peptide-polyketide antitumor drug bleomycin. Chem. Biol. *8*, 725–738.

Simunovic, V., and Müller, R. (2007a). Mutational analysis of the myxovirescin biosynthetic gene cluster reveals novel insights into the functional elaboration of polyketide backbones. ChemBioChem *8*, 1273–1280.

Simunovic, V., and Müller, R. (2007b). 3-Hydroxy-3-methylglutaryl-CoA-like synthases direct the formation of methyl and ethyl side groups in the biosynthesis of the antibiotic myxovirescin A. ChemBioChem *8*, 497–500.

Singh, R., Sharma, M., Joshi, P., and Rawat, D.S. (2008). Clinical status of anticancer agents derived from marine sources. Anticancer Agents Med. Chem. *8*, 603–617.

Smith, S., and Tsai, S.C. (2007). The type I fatty acid and polyketide synthases: a tale of two megasynthases. Nat. Prod. Rep. *24*, 1041–1072.

Staunton, J., and Weissman, K.J. (2001). Polyketide biosynthesis: a millennium review. Nat. Prod. Rep. *18*, 380–416.

Steussy, C.N., Vartia, A.A., Burgner, J.W., II, Sutherlin, A., Rodwell, V.W., and Stauffacher, C.V. (2005). X-ray crystal structures of HMG-CoA synthase from *Enterococcus faecalis* and a complex with its second substrate/inhibitor acetoacetyl-CoA. Biochemistry *44*, 14256–14267.

Steussy, C.N., Robison, A.D., Tetrick, A.M., Knight, J.T., Rodwell, V.W., Stauffacher, C.V., and Sutherlin, A.L. (2006). A structural limitation on enzyme activity: the case of HMG-CoA synthase. Biochemistry *45*, 14407–14414.

Sudek, S., Lopanik, N.B., Waggoner, L.E., Hildebrand, M., Anderson, C., Liu, H., Patel, A., Sherman, D.H., and Haygood, M.G. (2007). Identification of the putative bryostatin polyketide synthase gene cluster from "*Candidatus* Endobugula sertula", the uncultivated microbial symbiont of the marine bryozoan *Bugula neritina*. J. Nat. Prod. *70*, 67–74.

Sun, M.-K., Hongpaisan, J., and Alkon, D.L. (2009). Postischemic PKC activation rescues retrograde and anterograde long-term memory. Proc. Natl. Acad. Sci. USA *106*, 14676–14680.

Theisen, M.J., Misra, I., Saadat, D., Campobasso, N., Miziorko, H.M., and Harrison, D.H. (2004). 3-hydroxy-3-methylglutaryl-CoA synthase intermediate complex observed in "real-time". Proc. Natl. Acad. Sci. USA *101*, 16442–16447.

Weissman, K.J. (2009). Introduction to polyketide biosynthesis. Methods Enzymol. *459*, 3–16.

Wu, K., Chung, L., Revill, W.P., Katz, L., and Reeves, C.D. (2000). The FK520 gene cluster of *Streptomyces hygroscopicus var. ascomyceticus* (ATCC 14891) contains genes for biosynthesis of unusual polyketide extender units. Gene *251*, 81–90.

Wu, J., Cooper, S.M., Cox, R.J., Crosby, J., Crump, M.P., Hothersall, J., Simpson, T.J., Thomas, C.M., and Willis, C.L. (2007). Mupirocin H, a novel metabolite resulting from mutation of the HMG-CoA synthase analogue, *mupH* in *Pseudomonas fluorescens*. Chem. Commun. (Camb.) *20*, 2040–2042.

